Inflammation in the pleural cavity following injection of multi-walled carbon nanotubes is dependent on their characteristics and the presence of IL-1 genes

Yke Jildouw Arnoldussen, Vidar Skaug, Mona Aleksandersen, Erik Ropstad, Kristine Haugen Anmarkrud, Elin Einarsdottir, Fang Chin-Lin, Cesilie Granum Bjørklund, Mayes Kasem, Einar Eilertsen, Ron N. Apte & Shanbeh Zienolddiny

ARTICLE

Inflammation in the pleural cavity following injection of multi-walled carbon nanotubes is dependent on their characteristics and the presence of IL-1 genes

Yke Jildouw Arnoldussen[a]*, Vidar Skaug[a], Mona Aleksandersen[b], Erik Ropstad[c], Kristine Haugen Anmarkrud[a], Elin Einarsdottir[a], Fang Chin-Lin[a], Cesilie Granum Bjørklund[c], Mayes Kasem[a], Einar Eilertsen[a], Ron N. Apte[d] and Shanbeh Zienolddiny[a] [ID]

[a]Department of Biological and Chemical Work Environment, National Institute of Occupational Health, Oslo, Norway; [b]Department of Basic Sciences and Aquatic Medicine, Faculty of Veterinary Medicine, Norwegian University of Life Sciences, Oslo, Norway; [c]Department of Production Animal Clinical Sciences, Faculty of Veterinary Medicine, Norwegian University of Life Sciences, Oslo, Norway; [d]The Shraga Segal Department of Microbiology, Immunology, and Genetics, The Faculty of Health Sciences, Ben Gurion University of the Negev, Beer Sheva, Israel

ABSTRACT

Upon inhalation, multi-walled carbon nanotubes (MWCNTs) may reach the subpleura and pleural spaces, and induce pleural inflammation and/or mesothelioma in humans. However, the mechanisms of MWCNT-induced pathology after direct intrapleural injections are still only partly elucidated. In particular, a role of the proinflammatory interleukin-1 (IL-1) cytokines in pleural inflammation has so far not been published. We examined the MWCNT-induced pleural inflammation, gene expression abnormalities, and the modifying role of IL-1α and β cytokines following intrapleural injection of two types of MWCNTs (CNT-1 and CNT-2) compared with crocidolite asbestos in IL-1 wild-type (WT) and IL-1α/β KO (IL1-KO) mice. Histopathological examination of the pleura 28 days post-exposure revealed mesothelial cell hyperplasia, leukocyte infiltration, and fibrosis occurring in the CNT-1 (Mitsui-7)-exposed group. The pleura of these mice also showed the greatest changes in mRNA and miRNA expression levels, closely followed by CNT-2. In addition, the CNT-1-exposed group also presented the greatest infiltrations of leukocytes and proliferation of fibrous tissue. WT mice were more prone to development of sustained inflammation and fibrosis than IL1-KO mice. Prominent differences in genetic and epigenetic changes were also observed between the two genotypes. In conclusion, the fibrotic response to MWCNTs in the pleura depends on the particles' physico-chemical properties and on the presence or absence of the IL-1 genes. Furthermore, we found that CNT-1 was the most potent inducer of inflammatory responses, followed by CNT-2 and crocidolite asbestos.

Introduction

Due to their specific properties, manufactured carbon nanotubes (CNTs) have emerged as very applicable nanomaterials in a variety of commercial products. CNTs are biopersistent structures made of carbon with fibrous structures that vary in length, width, rigidity, number of walls (single or multi-walled), chemical composition, surface reactivity, and the presence of other elements than carbon. There is, however, a major concern about anticipated health effects notably in workers exposed to some of the CNTs. The various CNT characteristics such as their structure, length, aspects ratio, surface area, degree of aggregation, extent of oxidation, bound functional group, method of manufacturing, concentration and dose, contribute to their possible unwanted and pathological effects, whereof the long CNTs, their rigidity and biodurability have been of major concern (Poland et al., 2008; Donaldson et al., 2006).

Subsequent to pharyngeal aspiration of multi-walled CNTs (MWCNTs) in mice, CNTs are translocated to the subpleural tissue and intrapleural

space, depending on the length of the fibers (Mercer et al., 2010). Similarly, after intratracheal (i.tr.) instillation, long MWCNTs translocated more readily than the shorter ones from the lung to the pleural space, and only long fibers were associated with inflammatory responses and hyperplastic visceral mesothelial proliferation (Xu et al., 2012). Following intrapleural (i.pl.) injection, long amosite asbestos fibers, and long MWCNTs were less easily cleared through stomata in the parietal pleura resulting in a length-dependent retention in the pleura, and induction of inflammation leading to progressive fibrosis, which was not observed for short MWCNTs (Murphy et al., 2011). The mechanisms of translocation from the lung to the pleura still remain unclear. In lung tissue, MWCNTs instilled via the i.tr. route also elicited early inflammatory responses, DNA damage, and more fibrosis compared to short MWCNTs (Poulsen et al., 2015). The acute and chronic responses in the lung were found in conjunction with changes in gene and protein expression (Erdely et al., 2009; Poulsen et al., 2013; Poulsen et al., 2015). A recent study showed elevated expression of the proinflammatory cytokines tumor necrosis factor-α (TNF-α), IL-1α, IL-1β, IL-6, and C-C motif chemokine ligand-2 (CCL-2) in lung tissues, as well as bronchoalveolar lavage from mice exposed to MWCNTs by pharyngeal aspiration (Dong et al., 2015).

Although there is increasing evidence for the role of inflammatory responses in MWCNT-induced inflammation, fibrosis, and tumorigenesis, the understanding of molecular mechanisms involved is still incomplete. Several studies show the importance of IL-1 signaling in tissue and cell responses to MWCNTs. We have previously shown that cells with intact IL-1 signaling were much more prone to the toxic effects of the MWCNTs than IL1-KO cells, although differences were observed depending on the type of MWCNT (Arnoldussen et al., 2015).

The peritoneal lining has been used in rodents as proxy for pleural mesothelium in mechanistic studies of high aspect ratio nanomaterial (HARN)-induced lesions. Rodents intraperitoneally injected with MWCNTs developed inflammation and fibrosis (Donaldson and Poland, 2009) and malignant mesothelioma in the peritoneal mesothelial linings (Vaslet, Messier, and Kane 2002; Takagi et al., 2012). Comparative studies on effects of the i.pl. and i.p.

exposure routes to MWCNTs are not available. However, some differences between the two have been shown in the pathology of mesotheliomas induced by asbestos (Davis et al., 1986). MWCNT can reach the subpleura in mice after single and short-term inhalation exposures (Ryman-Rasmussen et al., 2009). A most recent review of carcinogenicity of CNTs showed that exposure of rodents through various exposure routes including inhalation led to the formation of mesotheliomas and lung carcinomas (Fukushima et al., 2018). These and other studies show that the pleura is the main site for mesothelial pathologies caused by asbestos and other similar fibrous structures when exposed by inhalation and directly to cavities lined by mesothelium. Moreover, MWCNTs reaching the lung parenchyma via airways may translocate to the pleura. It has also been shown that single and strait fibers were more effectively translocated from lung to pleural space and that formation of mesotheliomas may be related to the presence of these fibers (Kasai et al., 2016). We therefore used i.pl. injection as a relevant route to investigate directly the effects of the MWCNTs in pleural tissues to investigate the effects of MWCNTs and asbestos in the pleura after 28 days focusing on histopathological alterations and mRNA and miRNA expressions, with specific focus on the effects of the different MWCNTs compared to asbestos. To evaluate a possible role for IL-1 cytokines, we chose IL1-KO mice lacking IL-1α and IL-1β. These mice have been shown to be more resistant to chemical carcinogenesis compared to IL1-WT mice (Krelin et al., 2007). Possible differences in parietal pleural responses between WT and IL1-KO mice were investigated both at the histopathological and biomolecular levels, and similarly for the lung tissue responses in the same animals.

Materials and methods

Animals

The C57BL/6 IL1α/β double knockout mice were obtained from Professor Ron N. Apte (Ben Gurion University, Beer-Sheva, Israel) (Horai et al., 1998; Krelin et al., 2007) and were back-crossed with WT C57BL/6 mice (Charles River Lab., New York, NY) to obtain heterozygotes and IL1$\alpha^{-/-}\beta^{-/-}$ homozygous and WT mice. The study was performed at the Section for Experimental Biomedicine at

The Norwegian University of Life Sciences in Oslo, Norway. The unit is licensed by the Norwegian Animal Research Authority (NARA) and accredited by Association for Assessment and Accreditation of Laboratory Animal Care (www.aaalac.org). The study was approved by the unit's animal ethics committee (Institutional Animal Care and Use Committee/IACUC; FOTS: 6324) and NARA (2014/59831-2).

Preparation and dispersion of the test substances in dispersion medium

MWCNTs used in this study were Mitsui-7 (CNT-1) and n-Tec (CNT-2) in addition to UICC crocidolite asbestos that was used for comparison (Timbrell, Gibson, and Webster 1968). The materials have been characterized previously and dispersed as described before (Arnoldussen et al., 2015). Main characteristics are shown in Supplementary Table S1 and Supplementary Figure S1. The observations of fibers morphology by SEM showed that a majority of both CNTs fiber groups were single and strait. The total number concentration of CNT-1 was 2.8×10^6 fibers/μg material, whereof 1.5×10^6 fibers/μg were single and strait. The corresponding concentrations for CNT-2 were respectively 14.5×10^6 and 12.9×10^6 fibers/μg material. In both CNTs groups, a fraction of fibers was present as bundles or tangled. The SEM analysis also showed that CNT-2 had less bundles or bent and tangled fiber morphologies. Postmortem observation of the fibers in pleural lavage could give a more realistic picture of the fiber morphologies, however, we did not investigate pleural fluid with SEM to look for particle morphologies in the pleural fluid.

Intra-pleural injection (i.pl) of the MWCNTs and asbestos

Groups of six or seven C57BL/6 WT or IL1-KO mice were injected under anesthesia through the right chest wall to the pleural space with 100 μl of dispersion medium (DM) alone (sham exposed), 100 μl of DM containing 50 or 100 μg of CNT-1, CNT-2, or crocidolite asbestos (Supplementary Table S2).

Euthanasia, collection, and preparation of biological samples for histology and gene expression

Euthanasia was performed at day 28 by short exposure to CO_2, followed by the opening of the thorax, and removal of the trachea and lungs in one piece. Pieces of the left lung were sampled for histology and RNA analysis as depicted in Supplementary Figure S2. For histology, the tissue was trimmed and embedded in paraffin. For gene expression, the tissue piece was immersed in RNA-Later solution.

The diaphragm covered by the pleura was cut in two equal halves; hereof one was fixed in formalin under slight pressure in a tissue cassette overnight, then cut into longitudinal tissue strips and embedded upright in the paraffin block. Three tissue sections of 3 μm thickness both from lung and pleura were cut and mounted on a glass slide for histopathological examination.

The other half was immediately immersed in RNA-later for miRNA/mRNA expression analysis.

Histological examination

HE and HES (hematoxylin–eosin–safranin)-stained histological slides from the pleura and lungs were examined by light microscopy. The pleura were examined for (a) the presence of fibers, (b) leukocyte infiltration, (c) proliferation of fibrous tissue, (d) mesothelial cell hyperplasia, and (e) presence of granulomas. Lesions were assessed semi-quantitatively for each animal using a scoring system ranging from 0 (no changes) to 4 (severe changes).

Genetic and epigenetic analyses

Total RNA was extracted from tissue samples and used to synthesize cDNA for use in quantitative PCR (qPCR). To analyze the mRNA expression simultaneously of many genes involved in fibrosis, we used RT^2 Profiler^{TM} PCR Array Mouse Fibrosis #PAMM-120Z (SaBiosciences, Qiagen). A similar approach was used to investigate miRNA expression using the Mouse Fibrosis miScript miRNA PCR Array #MIMM-117ZE (SaBiosciences, Qiagen).

Statistical analyses

Gene expression data were analyzed using t-test and nonparametric Mann–Whitney test as appropriate. To test the effect of test particle exposures on inflammatory outcome variables, semi-quantitative measures of histopathological changes were treated

as continuous variables. Analyses were performed using JMP®, Version 12.1.0 (SAS Institute Inc., Cary, NC). General Linear Models were employed with fiber type, mouse strain, and the nested effect of fiber dose within fiber type as independent variables and amounts of fibers, inflammatory cells, progression of fibrosis, and number of granulomas in histological tissues as dependent variables. Least squares analysis was used to estimate effects of independent variables. *Post hoc* analyses were carried out using Tukey's multiple comparison test. Significance was assessed at $p < 0.05$.

More detailed information on materials and methods can be found in the Supplementary Materials and Methods file.

Results

Animal body weights and observations

WT mice decreased in weight for both doses for the CNTs and for 100 μg of crocidolite asbestos. A weight reduction was observed for IL1-KO control mice, whereas the weight increased in the CNT-injected mice. Animals were observed twice daily and there were no signs of abnormal respiration or discomfort. After 2 weeks and beyond, there was a steady increase in weight (Supplementary Figure S3).

Necropsy and gross pathology

On opening the thoracic walls, the pleural spaces were most affected in the high dose groups of CNT-1, consisting of variable amounts of pleural fluid, some hemorrhagic and others fibrinous. Some CNTs were observed freely in the fluid and others were seen on the parietal pleura and occasionally at the injection sites of the thoracic wall. In this CNT-1 group, the pleural linings were also in general clearly more affected than in others, presenting fibrous adhesions between the two pleural layers and in some increased thickness of the diaphragm with adhesions involving the adjacent lung. Fibrinous exudates were also observed in the visceral pleura of the lungs, and some focal patches with thickening. Both the chest wall pleura and the thickened pleura on the diaphragm presented patchy areas with agglomerated CNTs. The CNT-2 group presented identical changes but to a lesser extent. For the asbestos-exposed group, bluish fibers were not seen as frequently as the black fibers in the CNT-1 group. The asbestos-exposed animals had the least macroscopic changes. At the gross level, we were not able to distinguish between KO and WT mice. Apart from lung and pleura, other organs were essentially unaffected.

Histopathological changes

Exposed animals showed several pathological lesions in the pleura. Lesions included accumulation of MWCNT or asbestos fibers, fibrosis, infiltration with mononuclear cells, granulomas, and hyperplasia of mesothelial cells. A summary of the extent of the presence of fibers and histopathological observations for the pleura is shown in Table 1. The animals in the CNT-1 groups and the CNT-2 high-dose group had generally, more severe lesions than the CNT-2 low-dose group and the crocidolite asbestos groups, when compared to the unexposed control animals. Among the exposed groups, animals injected with the CNTs had significantly more inflammatory cell infiltration than the mice injected with crocidolite asbestos (Table 1). The lesions in the parietal pleura were characterized by multifocal to confluent granulomatous inflammation and were in the visceral pleura more severe in the cranioventral parts than the caudodorsal parts. Fibrosis in the pleura was significantly increased in all exposed

Table 1. Overall effects of fibers independent of genotype.

Exposure	Presence of fibers		Infiltration of inflam. cells		Granulomas		Fibrotic responses	
	LS Mean	SE	LS Mean	SE	LS Mean	SE	LS Mean	SE
CONTROL	0.0 d	0.26	0.0 c	0.20	0.0 c	0.24	0.0 c	0.25
CROC	1.0 c	0.20	2.4 b	0.20	1.2 b	0.17	2.2 b	0.19
CNT-2	2.0 b	0.18	2.2 b	0.20	1.8 b	0.17	2.4 b	0.17
CNT-1	3.0 a	0.18	3.1 a	0.20	3.6 a	0.17	3.6 a	0.18

Least Square Means (LS Mean) of semiquantitative scores (Grading 0–4) for the independent variables: presence of fibers, infiltration of inflammatory cells, granulomas, and fibrotic responses, in pleura of mice exposed to sham, crocidolite asbestos, CNT-2, or CNT-1, respectively. Levels not connected by the same letter (a, b, c, or d) are significantly different.

groups when compared with the control group (Table 1, Figure 1). Among the CNT exposed groups, pleural lesions were more severe in the CNT-1 exposed animals (Table 1, Figure 2(A,C,D)) and milder in the CNT-2 group and in the asbestos-exposed groups (Figures 2(B) and 3(A,B)). Granulomas with numerous giant cells, epithelioid cells, macrophages, and fibers were often observed in mediastinum and pleura (Figure 2(A,D)) and were more numerous in the CNT-1 groups than the other exposed groups (Table 1). Moreover, fibrous adhesions were often observed between the parietal and visceral pleura less often involving the subjacent lung tissue, and between lung lobes (Figure 2(A,C)).

Inflammatory cell infiltrates present in pleura were dominated by macrophages, lymphocytes, plasma cells, epithelioid cells, and multinucleated giant cells (Figures 2(B,D) and 3(A,B)). CNT fibers and crocidolite asbestos fibers were observed in extracellular and intracellular locations and were more numerous inside granulomas (Figure 3(A)). Accumulation of fibers was notably higher in the CNT-1-exposed group than in the CNT-2 or asbestos-exposed groups. The mesothelium of visceral pleura showed multifocal hyperplasia with small nests and rows of proliferated cells in all exposed animals (Figure 3(B)). There was less inflammatory cell infiltrates in the pleura of the IL1-KO mice than in WT mice. The presence of granulomas did not differ significantly between WT and IL1-KO mice.

Lung lesions were present in some mice in all the exposed groups and included focal infiltration of leukocytes and fibrosis (Figure 2(B)). In a small number of animals in the CNT-1, high dose group
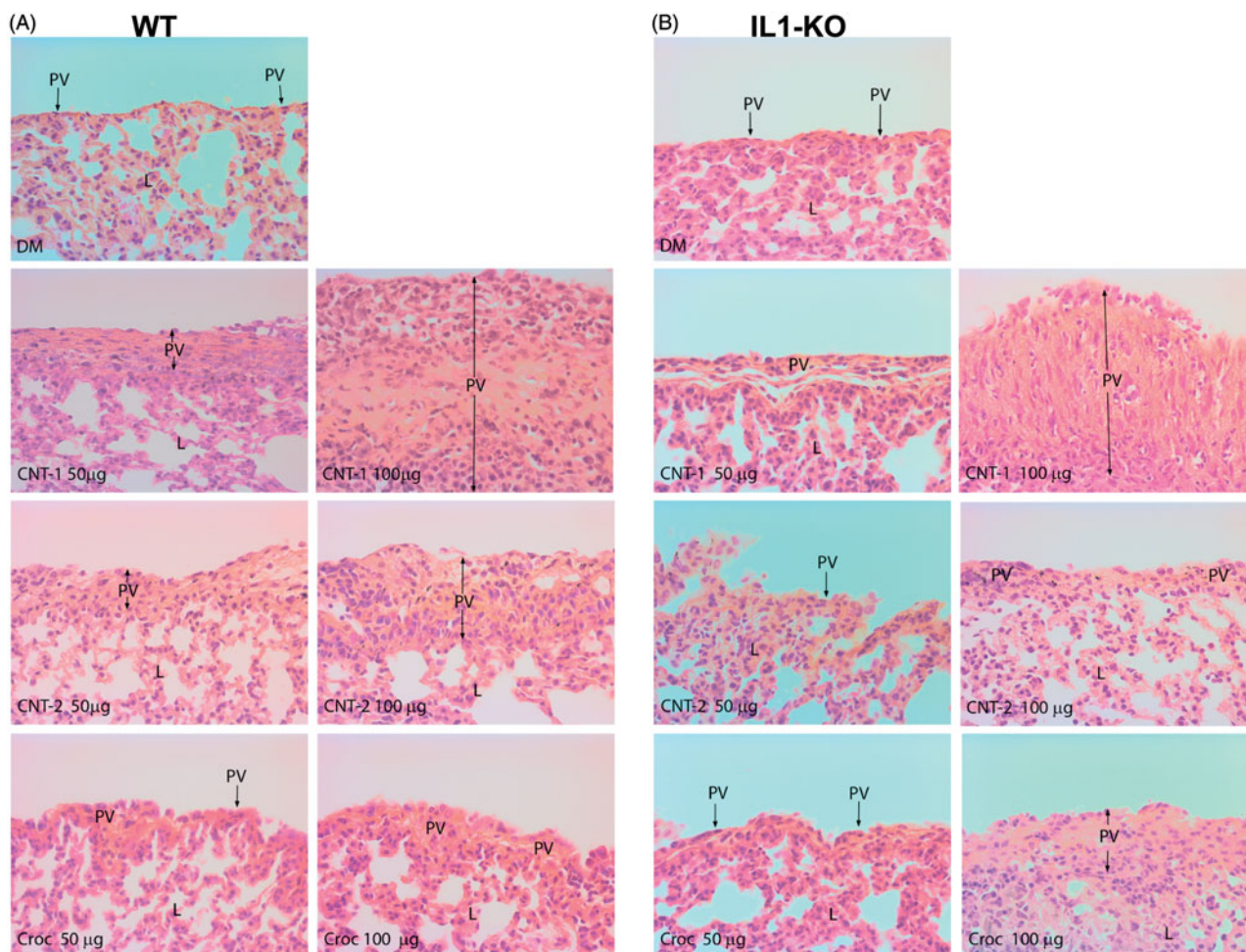
Figure 1. Pleural fibrosis in WT and IL1-KO mice. (A) Lesions of visceral pleura (PV and arrows) in WT mice. Fibrosis and inflammatory cells are present in PV of all exposure groups. Collagen fibers (stained in yellow-orange) are more abundant in PV of the high CNT groups. L = lung. The sections were stained with HES and a magnification of 400× is shown for all photographs. (B) Lesions of visceral pleura (PV and arrows) in IL1-KO mice. Fibrosis and inflammatory cells are present in PV of all exposure groups. Collagen fibers (stained in yellow-orange) appear to be more abundant in the CNT-1 and crocidolite asbestos high exposure groups. L: lung. The sections were stained with HES and a magnification of 400× is shown for all photographs.
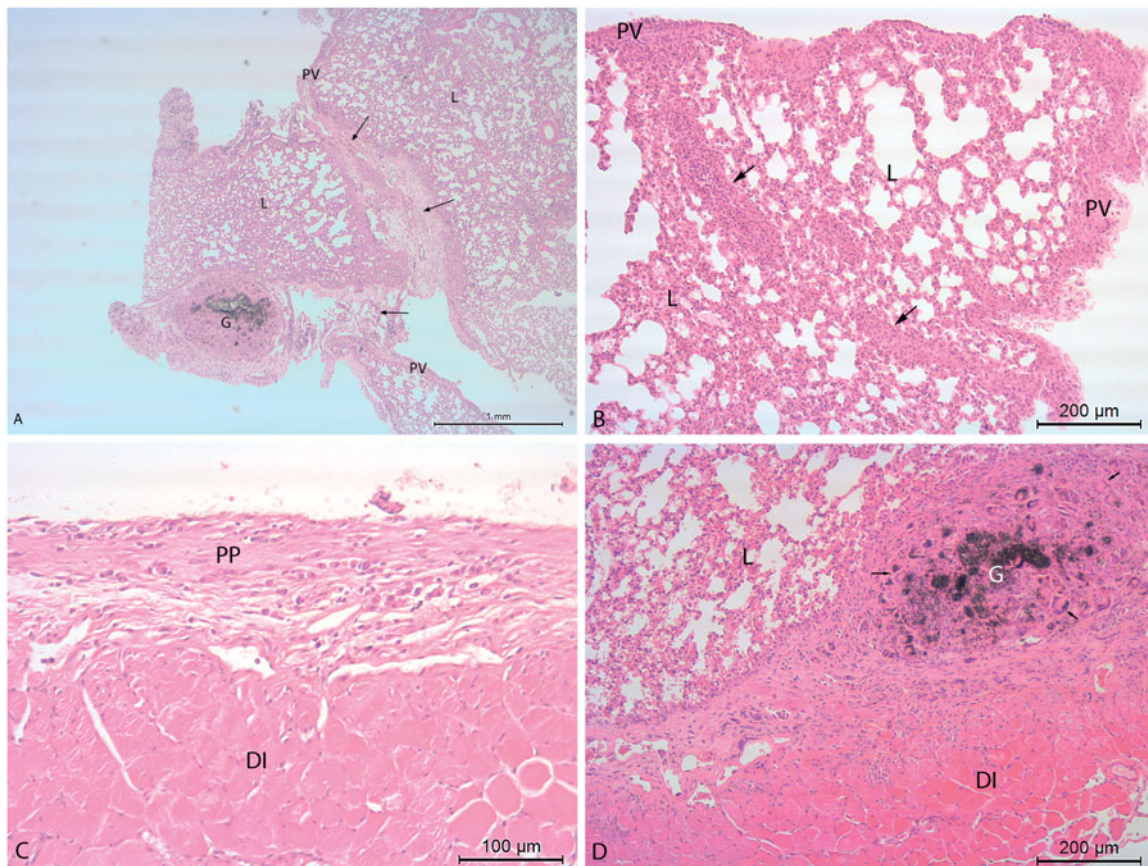
Figure 2. Induction of pleural lesions by the CNTs and crocidolite asbestos. (A) Chronic pleuritis with thickened visceral pleura (PV), fibrous adhesions between lung lobes (arrows) and granuloma formation (G) in a WT mouse exposed to 100 μg CNT-1. HE stain. (B) Visceral pleura (PV) is thickened due to infiltration of inflammatory cells, fibroplasia, and proliferation of mesothelial cells. In the lungs (L), the fibrous septa are thickened and infiltrated with inflammatory cells (arrows). IL1-KO mouse exposed to 50 μg crocidolite asbestos. HE stain. (C) Parietal pleura (PP) with proliferation of fibrous tissue and moderate infiltration of mononuclear inflammatory cells in an IL1-KO mouse exposed to 50 μg CNT-1. D: diaphragm. HE stain. (D) Fibrous adhesions between lungs (L) and diaphragm (D) with a large granuloma (G) in pleura. IL1-KO mouse exposed to 100 μg CNT-1. HE stain.
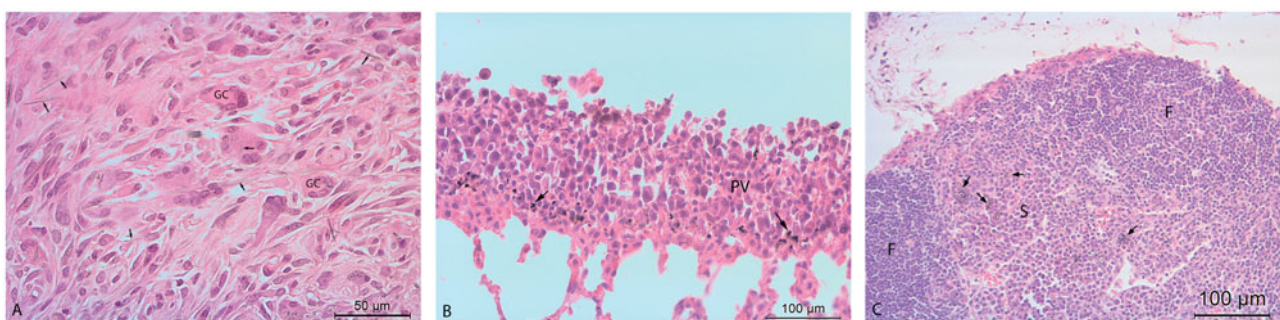
Figure 3. Inflammatory cell infiltration and fiber accumulation. (A) Granuloma of a WT mouse exposed to 100 μg crocidolite asbestos. The granuloma contains numerous giant cells (GC) and macrophages. Many asbestos fibers are present (arrows). HE stain. (B) Visceral pleura (PV) with distinct proliferation of mesothelial cells in an IL1-KO mouse exposed to 100 μg CNT-2. Black CNT-2 fibers are present (arrows). HE stain. (C) Mediastinal lymph node from an IL1-KO mouse exposed to 100 μg CNT-1 with reactive hyperplasia. The sinus and paracortex (S) contains numerous histiocytic cells of which some contain fibers (arrows). F = lymph node follicles. HE stain.

fibers and granulomas were present in the lung tissues. A reactive hyperplasia was present in the mediastinal lymph nodes of several exposed animals and fibers were usually found in these lymph nodes (Figure 3(C)). Focal myositis with the presence of fibers was observed in the diaphragm in some mice.

Dose–effect relationship of fiber dose

The effect of dose nested within exposure group was significant for the outcome variables granulomas, amount of fibrosis, inflammatory cells, and fibers in the pleura. Generally, high dose exposed animals showed higher scores.

Signature of CNTs on gene expression in the pleura and lung

To identify the signature of the CNTs on gene expression, a mouse fibrosis-specific array was used to investigate the expression of 84 genes involved in fibrosis. Analysis of the array results indicated most differences in gene expression of genes in the pleura (Supplementary Table S3). Of the 84 genes, 42 genes displayed interesting up- or down-regulation either between the different types of exposures or between WT and IL1-KO mice. From these, 12 genes (*Ccl12*, *Ccl3*, *Col1a2*, *Col3a1*, *Cxcr4*, *Lox*, *Mmp13*, *Mmp9*, *Serpina1a*, *Timp1*, *Timp4*, and *Bcl2*) that were highly regulated were chosen for further quantitative analysis by qPCR in pleura and lung tissue from each individual mouse.

The three exposure types had different impact on the expression of the various genes. The fold regulation for each investigated gene was calculated and compared for exposed and non-exposed control mice for CNT-1, CNT-2, and crocidolite asbestos (Table 2). CNT-1 clearly had the most significant impact on gene expression for both 50 and 100 μg in pleura from WT mice (Table 2(A)). All genes, except *Serpina1a*, *Timp4*, and *Bcl2* were upregulated after CNT-1 exposure. CNT-2 also had a large impact on gene regulation inducing significant changes in nine of the 12 genes (Table 2(A)). Of these only *Serpina1a* and *Timp4* were clearly downregulated. Asbestos had the lowest impact and 100 μg had a higher impact on gene expression than 50 μg. Genes upregulated in the pleura from

Table 2. Fold changes in gene expression of CNT or asbestos exposed WT and IL1-KO mice versus control exposed mice.

mRNA/Exposure	CNT-50	CNT-100	CNT-2 50	CNT-2 100	Croc 50	Croc 100
(A) Pleura, WT						
Ccl12	3.85	7.23	1.86	2.44	3.30	1.78
Ccl3	33.53	80.68	17.06	21.88	9.48	26.71
Col1a2	3.04	3.11	1.45	1.76	1.20	1.21
Col3a1	1.59	1.69	−1.06	1.18	−1.04	1.02
Cxcr4	1.89	2.09	1.43	1.69	−1.04	1.78
Lox	1.79	1.70	−1.44	−1.45	−1.39	−2.03
Mmp13	4.91	10.40	1.44	1.68	1.40	1.93
Mmp9	2.30	1.70	1.83	2.15	1.47	2.64
Serpina1a	−10.60	−13.38	−2.85	−8.34	−1.11	1.22
Timp1	12.72	16.05	2.66	3.18	3.41	3.25
Timp4	−4.90	−5.22	−1.83	−1.86	−1.30	−6.75
Bcl2	−1.46	−1.52	1.03	1.00	−1.06	−1.21
(B) Pleura, KO						
Ccl12	5.93	7.82	2.00	2.55	2.67	5.09
Ccl3	17.96	21.77	4.69	5.08	2.85	3.29
Col1a2	2.79	2.81	−1.53	1.06	−1.05	−1.40
Col3a1	1.74	1.60	−1.65	−1.05	−1.04	−1.14
Cxcr4	1.68	1.37	−1.21	−1.25	−1.34	−1.44
Lox	2.68	2.79	−1.20	1.07	1.55	−1.05
Mmp13	4.57	8.02	1.20	−1.03	1.02	−1.26
Mmp9	1.03	1.30	1.27	−1.01	1.01	−1.56
Serpina1a	−5.24	−2.12	2.30	−55.36	−1.13	−2.50
Timp1	11.90	10.60	1.19	1.32	1.32	2.94
Timp4	−2.55	−3.40	−1.25	−1.40	1.28	−2.62
Bcl2	−1.94	−2.24	−1.23	−1.47	−1.23	−1.78
(C) Lung, WT						
Ccl12	1.94	3.17	1.00	1.20	1.32	1.00
Ccl3	1.72	2.31	2.16	1.71	1.17	1.87
Col1a2	1.32	1.98	1.08	1.16	1.01	1.05
Col3a1	1.27	2.23	1.31	1.26	1.32	1.23
Cxcr4	−1.06	−1.09	1.04	1.16	−1.06	1.10
Lox	−1.77	−1.15	−1.26	−1.67	−1.42	−1.92
Mmp13	−1.13	1.26	−1.07	1.05	1.05	−1.10
Mmp9	1.27	1.33	1.38	1.24	1.17	1.37
Serpina1a	nd	nd	nd	nd	nd	nd
Timp1	4.38	5.53	1.75	1.87	1.80	1.95
Timp4	−1.35	−1.88	1.16	1.06	1.06	1.10
Bcl2	−1.38	−1.34	−1.18	−1.15	−1.20	−1.20

(*continued*)

(D) Lung, KO						
Ccl12	2.72	1.71	−1.33	1.00	2.09	1.37
Ccl3	1.77	2.06	1.74	2.29	1.47	1.58
Col1a2	1.65	1.58	−1.05	−1.05	1.01	1.05
Col3a1	1.51	1.15	−1.34	−1.28	1.26	1.26
Cxcr4	1.07	1.08	1.28	1.32	1.06	1.13
Lox	−1.37	−1.49	−1.46	−1.11	1.14	−1.32
Mmp13	1.34	1.21	1.42	1.88	−1.01	1.02
Mmp9	1.02	1.55	1.62	2.33	1.26	−1.15
Serpina1a	nd	nd	nd	nd	nd	nd
Timp1	3.94	3.39	0.81	0.89	1.54	1.60
Timp4	−1.64	−1.31	−1.24	1.13	−1.04	−1.28
Bcl2	−1.45	−1.44	−1.11	1.00	−1.11	−1.25

Results are shown for (A) pleura WT, (B) pleura IL1-KO, (C) lung WT, and (D) lung IL1-KO. Significant differences from the controls ($p < 0.05$) are marked in color where light green = positive fold regulation up to 5, dark green = positive fold regulation higher than 5, light red = negative fold regulation down to −5, dark red = negative fold regulation lower than −5. Non-detected expression is annotated by nd.

WT mice in response to all test substances were *Ccl12*, *Ccl3*, *Mmp9*, and *Timp1* (Table 2(A)). Particle exposures induced less significant changes in gene expression of IL1-KO mice (Table 2(B)). Both doses of CNT-1 had the highest impact, whereas CNT-2 and asbestos had limited effects where only the highest dose of 100 μg had the most significant impact. Again, *Ccl12*, *Ccl3*, and *Timp1* were among the genes with the highest induced upregulation, whereas *Serpina1a*, *Timp4*, and *Bcl2* were downregulated (Table 2(B)).

The two CNTs and asbestos had less significant effects on changes in gene expression in lung tissue from WT and IL1-KO mice (Table 2(C,D)). Despite this, CNT-1 induced more significant changes than CNT-2 and asbestos and affected genes such as *Ccl12*, *Ccl3*, and *Timp1*. Similar to pleura tissue, *Timp4* and *Bcl2* were downregulated, in addition to *Lox* (Table 2(C,D)).

Comparison of mRNA expression between WT and IL1-KO mice

Differences in gene expression between WT and IL1-KO mice for each of the exposure groups in pleura and lung tissue were investigated. The most significant changes were found for asbestos 100 μg, followed by CNT-2 and control exposure groups in pleural tissue (Table 3(A)). In general, most of the significant changes showed a downregulation of the fibrosis specific genes in IL1-KO mice (Table 3(A)). For lung tissue, the highest dose of both CNT-1 and CNT-2 had the most significant changes in gene expression (Table 3(B)).

Epigenetic signature of CNTs on miRNA expression in the pleura and lung

Epigenetic changes, namely, miRNA expression, in pleura and lung tissues from the mice were examined using an array of 84 miRNAs involved in fibrosis. Based on the fold change induced by each type of exposure compared to controls (Supplementary Table S4), nine miRNAs, *miR-1a*, *miR-133a*, *miR-146b*, *miR-19a*, *miR-19b*, *miR-200a*, *miR-200b*, *miR-205*, and *miR-874*, were chosen for further expression analysis in each individual mouse. As for gene expression analysis, the fold regulation for each miRNA was calculated between exposed and control mice (Table 4).

For the pleura, both doses of CNT-1, CNT-2, and asbestos had significant effects in WT mice. Significant downregulation with CNT-1 or CNT-2 exposure was observed for *miR-1a*, *miR-133a*, *miR-200a*, and *miR-200B*, whereas *miR-146b*, *miR-205*, and *miR-874* were significantly upregulated (Table 4(A)). The highest dose of asbestos had a significant effect on all of the tested miRNAs in WT mice but not in IL1-KO mice. Furthermore, CNT-1 had the largest effect in pleura tissue from IL1-KO mice (Table 4(B)).

For lung tissue, the effect of the exposures is small regarding miRNA expression in WT mice, whereas both CNTs induced large differences in IL1-KO mice. Surprisingly, *miR-146b* and *miR-205* are downregulated in lung tissue from IL1-KO mice (Table 4(D)) compared to the upregulation which was observed in pleura tissue from IL1-KO mice (Table 4(B)).

Comparison of miRNA expression between WT and IL1-KO mice

The highest dose of CNT-1 and asbestos had the most significant effects for pleura tissue (Table 5(A)).

Table 3. Fold changes in gene expression between IL1-KO and WT mice for each of the exposure groups.

mRNA/Exposure	CTRL	CNT-1 50	CNT-1 100	CNT-2 50	CNT-2 100	Croc 50	Croc 100
(A) Pleura							
Ccl12	1.11	1.40	−1.07	1.27	1.14	−1.06	2.73
Ccl3	2.43	1.15	−1.44	−2.49	−2.03	−1.33	−3.11
Col1a2	1.54	2.30	1.68	−1.25	1.07	1.46	−1.10
Col3a1	1.15	1.67	1.10	−1.13	1.18	1.50	1.13
Cxcr4	1.5	1.16	−1.10	−1.18	−1.62	1.08	−2.11
Lox	−1.47	1.14	1.04	−1.14	1.17	1.67	1.64
Mmp13	1.62	−1.09	−1.18	1.06	−1.78	1.02	−1.93
Mmp9	1.49	−1.79	1.12	−1.10	−1.61	−1.11	−2.95
Serpina1a	−2.94	−1.71	1.56	1.68	−6.50	−3.07	−11.71
Timp1	1.03	1.17	−1.41	−1.89	−1.84	−2.18	1.02
Timp4	−1.09	1.82	1.22	1.39	1.27	1.42	2.41
Bcl2	1.49	1.06	1.01	1.16	1.00	1.23	−1.06
(B) Lung							
Ccl12	−1.03	1.15	−1.95	−1.49	−1.23	1.50	1.21
Ccl3	1.10	1.07	−1.14	−1.29	1.45	1.25	−1.14
Col1a2	−1.09	1.14	−1.41	−1.19	−1.27	1.09	1.09
Col3a1	1.29	1.50	−1.55	−1.38	−1.22	1.20	1.22
Cxcr4	−1.05	−1.01	1.11	1.12	1.01	1.02	−1.09
Lox	−1.06	1.19	−1.48	−1.29	1.34	1.42	1.25
Mmp13	−1.15	1.36	−1.28	1.27	1.53	−1.29	−1.12
Mmp9	1.08	−1.19	1.28	1.16	2.06	1.10	−1.49
Serpina1a	nd	nd	nd	nd	nd	nd	nd
Timp1	1.25	1.13	−1.31	−1.68	−1.70	1.11	1.00
Timp4	1.18	−1.06	1.55	−1.31	1.14	1.02	−1.34
Bcl2	1.01	−1.05	−1.08	1.10	1.16	1.09	−1.04

Significant differences between the two genotypes ($p < 0.05$) are marked in color where light green = positive fold regulation up to 5, dark green = positive fold regulation higher than 5, light red = negative fold regulation down to −5, dark red = negative fold regulation lower than −5. Non-detected expression is annotated by nd.

However, for asbestos, all miRNAs were upregulated in IL1-KO mice compared to WT mice, whereas CNT-1 inhibits expression, except for *miR-205* and *miR-874* (Table 5(A)).

For lung tissue, the CNT-2 100 μg dose had the greatest impact on reducing expression in IL1-KO mice (Table 5(B)). When studying the differences between WT and IL1-KO mice, asbestos 100 μg had

Table 4. Fold changes in miRNA expression of CNT or asbestos exposed WT and IL1-KO mice versus control exposed mice.

miRNA/Exposure	CNT-1 50	CNT-1 100	CNT-2 50	CNT-2 100	Croc 50	Croc 100
(A) Pleura, WT						
miR-1a	−4.46	−2.44	−1.93	−1.93	−2.01	−8.44
miR-133a	−3.04	−3.25	−2.30	−2.72	−1.17	−2.99
miR-146b	7.81	9.24	5.28	7.81	1.45	2.38
miR-19a	−1.48	1.81	−1.71	1.16	−1.99	−4.87
miR-19b	−1.22	2.05	−1.25	1.58	−1.70	−3.91
miR-200a	−2.41	1.94	−1.52	−1.35	−4.06	−4.22
miR-200b	−1.89	3.30	−1.23	−1.09	−3.43	−2.62
miR-205	6.01	8.62	6.78	4.37	2.77	2.60
miR-874	1.21	1.23	1.76	1.24	−1.17	1.34
(B) Pleura, KO						
miR-1a	−1.84	−3.52	−1.34	1.28	−1.02	1.14
miR-133a	−1.47	−1.28	−1.13	1.09	−1.04	−1.38
miR-146b	7.33	5.24	1.14	2.05	1.47	4.29
miR-19a	1.35	−1.44	−2.52	−1.52	−1.23	−1.70
miR-19b	1.35	−1.72	−3.00	−1.71	−1.30	−1.80
miR-200a	−2.98	−4.88	−2.31	−1.47	−1.24	−1.32
miR-200b	−2.45	−2.80	−1.39	−1.38	−1.16	−1.15
miR-205	19.71	26.92	3.09	4.38	4.57	11.95
miR-874	1.87	2.08	1.27	1.79	−1.07	1.10
(C) Lung, WT						
miR-1a	−1.22	−1.39	1.02	−1.04	−1.33	1.10
miR-133a	1.26	−1.13	1.21	1.19	1.28	1.28
miR-146b	1.23	1.41	1.29	1.86	1.10	1.23
miR-19a	1.39	1.57	1.91	1.85	1.22	1.08
miR-19b	1.04	1.48	1.87	1.98	1.16	1.20
miR-200a	1.18	−1.07	1.02	1.04	1.05	1.05
miR-200b	2.03	1.51	1.63	1.84	1.17	1.43
miR-205	1.60	1.00	−1.07	1.17	1.23	1.05
miR-874	3.21	1.46	1.43	1.42	−1.05	1.31
(D) Lung, KO						
miR-1a	−3.23	−2.76	−3.37	−2.45	−1.25	−1.63
miR-133a	−2.27	−1.89	−2.02	−2.19	1.11	−1.29
miR-146b	−1.39	−1.46	−1.55	−1.56	−1.01	1.02
miR-19a	−1.52	−1.49	−1.30	−1.75	1.16	1.13
miR-19b	−1.43	−1.47	−1.26	−1.74	1.15	1.16
miR-200a	1.02	1.21	−1.13	−1.10	−1.03	1.08
miR-200b	1.04	1.43	1.10	−1.19	1.08	1.10
miR-205	−1.31	−1.28	−1.78	−1.78	1.11	−1.36
miR-874	3.22	4.07	2.32	1.96	1.52	1.35

Results are shown for (A) pleura WT, (B) pleura IL1-KO, (C) lung WT, and (D) lung IL1-KO. Significant differences from the controls ($p < 0.05$) are marked in color where light green = positive fold regulation up to 5, dark green = positive fold regulation higher than 5, light red = negative fold regulation down to −5, dark red = negative fold regulation lower than −5.

the largest significant effect on both gene and miRNA expression at the site of injection, the pleura, whereas the MWCNTs induce most differences in lung tissue.

Discussion

Several studies have addressed potential effects of MWCNTs on rodents and have shown that MWCNTs are toxic to the pleura and lungs following i.tr. instillation or exposure via airways (Mercer et al., 2010; Murphy et al., 2013; Porter et al., 2013; Kasai et al., 2015, 2016; Suzui et al., 2016; Fukushima et al., 2018). Likewise, several studies in vitro have shown that IL-1 signaling may also be important in cellular responses to nanomaterials in general, but the role of IL-1 in cellular responses of MWCNTs in the pleura has not been studied in vivo. It has been shown that MWCNTs can reach the subpleura and the pleural space in mice after a single and short time inhalation exposure (Ryman-Rasmussen et al., 2009; Xu et al., 2012; Porter et al., 2013), raising concerns that inhaled nanotubes may cause pleural fibrosis and/or mesothelioma. We therefore chose the i.pl. injection technique to investigate the direct effects of the particles on the mesothelium with a particular focus on the pleura and lung.

One week after i.pl. injection, the weight of WT mice injected with the MWCNTs decreased whereas the weight of IL1-KO mice increased compared to control exposed mice. A similar effect was only observed for the highest dose of asbestos. Both doses of CNT-1 had a major impact on the proliferation of mesothelial cells, leukocyte infiltration, and fibrotic lesions. In number metrics, over half of the fibrous materials in CNT-1 consisted of single fibers, but some fractions are bent or curved single fibers, in addition to small fiber bundles and fibrous clusters. The fibers of CNT-2 are shorter where about 90% of the fibrous material consisted of single and straight fibers (Arnoldussen et al., 2015). Previous studies have shown that long MWCNTs, similar to CNT-1 used here, and asbestos-induced acute inflammation and progressive fibrosis in parietal pleura, is probably due to length-dependent retention at the parietal pleura and that there is initially a more efficient clearance of short MWCNTs from the pleural cavity (Murphy et al., 2011, 2013). Moreover, statistical analyses of the effect of the

Table 5. Fold change in miRNA expression between IL1-KO and WT mice for each of the exposure groups.

miRNA/Exposure	CTRL	CNT-1 50	CNT-1 100	CNT-2 50	CNT-2 100	Croc 50	Croc 100
(A) Pleura							
miR-1a	−1.45	1.67	−2.10	−1.01	1.71	1.36	6.62
miR-133a	−2.11	−1.02	1.20	−1.04	1.40	−1.88	1.03
miR-146b	1.59	1.49	−1.11	−2.91	−2.40	1.61	2.86
miR-19a	−1.65	1.21	−4.32	−2.45	−2.91	−1.03	1.73
miR-19b	−1.19	1.39	−4.19	−2.84	−3.21	1.10	1.83
miR-200a	1.03	−1.19	−9.14	−1.47	−1.05	3.39	3.30
miR-200b	1.17	−1.11	−7.93	1.04	−1.08	3.46	2.68
miR-205	−1.11	2.96	2.81	−2.43	−1.11	1.49	4.15
miR-874	1.16	1.79	1.96	−1.20	1.67	1.27	−1.05
(B) Lung							
miR-1a	1.17	−2.27	−1.71	−2.84	−2.02	1.24	−1.54
miR-133a	1.54	−1.85	−1.09	−1.59	−1.70	1.34	−1.06
miR-146b	1.75	1.03	−1.18	−1.15	−1.66	1.57	1.45
miR-19a	1.23	−1.73	−1.90	−2.02	−2.64	1.17	1.29
miR-19b	1.36	−1.10	−1.60	−1.74	−2.53	1.35	1.31
miR-200a	−1.07	−1.24	1.21	−1.23	−1.22	−1.16	−1.04
miR-200b	1.53	−1.27	1.46	1.03	−1.42	1.42	1.18
miR-205	1.70	−1.24	1.33	1.02	−1.22	1.54	1.20
miR-874	1.00	1.00	2.77	1.61	1.37	1.59	1.03

Significant differences from the controls ($p < 0.05$) are marked in color where light green = positive fold regulation up to 5, dark green = positive fold regulation higher than 5, light red = negative fold regulation down to −5, dark red = negative fold regulation lower than −5.

fibers, independent of the mouse genotype, indicated that CNT-1 had the greatest impact followed by CNT-2 and crocidolite asbestos that had a very similar effect on the responses investigated by histopathology. As pointed out in a recent review by Fukushima et al. (2018), however, the effects of size and form of the CNTs related to their toxicological effects varies in various studies and requires further investigation.

The novelty of the present study is that it investigated the importance of IL-1 by using IL1-KO mice to study the effects of MWCNTs compared to crocidolite asbestos. We have previously shown that IL-1 may be important in the response to MWCNTs in vitro (Arnoldussen et al., 2015). Histopathological analysis indicated that IL1-KO mice were less prone to inflammation in the pleura than WT mice as there was a significantly reduced level of proliferation in the connective tissue and leukocyte infiltration. A role for and the importance of IL-1α in granuloma formation in the lungs has been demonstrated. It was shown that IL-1 deficient mice exposed to silica particles had reduced phagocytic macrophage accumulation and fewer granulomas

which were due to the absence of IL-1α, but not IL-1β (Huaux et al., 2015). In our study, by exploring granulomatous responses in pleura, there was a significant increase in response to both MWCNTs, in particular, CNT-1, and asbestos.

We consider the thin layer of connective tissue underlying the thin mesothelial lining cells and supported by the diaphragm, to be involved in the chronic inflammationrelated to the benign effects of the fibers in the pleura. Here we have shown that granulomas occur in all experimental groups, mostly in the highly pathogenic fiber group CNT-1, as a component of the inflammatory process. Our current understanding is that the main driving factor for these pleural effects is an underlying ongoing chronic inflammation induced by material–biological interaction. We are not aware of clear evidence for granulomas as such to precede a pre-cancerous lesion. This study was too short in time to identify any validated predictive markers of tumorigenesis. Future studies may clarify any hallmarks of inflammation to predict precancerous lesions. Therefore, we consider it is likely that the inflammatory reaction comes before the formation of benign and malignant pleural diseases, patchy focal areas of pleural fibrosis included. There was however, no difference between WT and IL1-KO mice and may suggest that a role for the IL-1 genes is dependent on the type and length of exposure.

To understand the molecular changes induced by MWCNT and asbestos exposure, gene expression was investigated. Fibrosis as an endpoint of exposure to MWCNTs and changes in gene expression have been reported in the lungs (Snyder-Talkington et al., 2013; Dong et al., 2015; Poulsen et al., 2015). Several interleukins were upregulated in WT mice. In addition to IL-1α and IL-1β that were increased in WT mice, IL-4 expression was increased in pleura from both WT and IL1-KO mice. Secretion of IL-4 triggers T2 helper cells, being part of the adaptive immune response, and is a key fibrosis mediator (Jakubzick et al., 2003). Moreover, as IL-4 is upregulated in IL1-KO mice after MWCNT exposure this indicates that its expression is not affected by the lack of IL-1. Members of the transforming growth factor (TGF) family were not affected by the MWCNTs. There is the possibility of an earlier upregulation immediately after MWCNT injection which is decreased after 28 days and was shown before

(Poulsen et al., 2015). From the more closely investigated genes, in particular, a significant upregulation of Ccl12, Ccl3, Mmp9, and Timp1 and a significant downregulation of Serpina1a, Timp4, and Bcl2 was observed for most of the exposure types.

Both Ccl12 and Ccl3 have important roles in the induction of fibrosis, including the recruitment of fibroblasts and regulation of macrophage recruitment and infiltration (Moore et al., 2006; Ishida et al., 2007). Changes were most apparent in pleural tissue from both WT and IL1-KO mice exposed to all three types of particles. IL-1 did not seem to play an important role in Ccl12 and Ccl3 expression, neither in pleura nor in the lung. Both of these genes were upregulated in lung tissue in the study by Poulsen et al. where two different MWCNTs designated as CNT$_{small}$ and CNT$_{large}$ induced Ccl12 and Ccl3 expression 1 and 3 days after intra-tracheal instillation with 18, 54, and 162 μg (Poulsen et al., 2015). After 28 days only 162 μg CNT$_{large}$ (resembling CNT-1 in our study) had an effect. Basis for these differences may lie in the different exposure techniques as both studies used C57BL/6 mice. Furthermore, Ccl3 was upregulated in the lungs from mice exposed to 1, 2, or 4 mg/kg MWCNT by oropharyngeal aspiration (Wang et al., 2011) further emphasizing a role for Ccl3 in fibrosis.

The family of matrix proteinases (MMPs) was upregulated in the WT mice. These are important for turnover and degradation of extracellular matrix (ECM) substrates but also mediate in immunity and repair such as cell migration, leukocyte activation, antimicrobial defense and chemokine processing (Manicone and McGuire, 2008; Pardo et al., 2016). The Mmp9 gene was upregulated by all exposure types, especially in pleural tissue from WT mice. A pro-fibrotic effect of Mmp9 was observed in various tissues such as lung, liver, and kidney (Pardo et al., 2016). Mmp9 was downregulated in IL1-KO injected with the highest doses of CNT-2 and asbestos in the pleura. It has been reported that MMP9 is augmented by IL-1β (Oh et al., 2008) and this may the reason for its downregulation in the pleura from IL1-KO mice. Moreover, the transcription factor specificity protein 1 (SP-1) is essential for Mmp9 transcription (Murthy et al., 2010) and as SP-1 was downregulated by CNT-1 in IL1-KO mice on the array, this may add to the observed downregulation in the pleura from IL1-KO mice. For the lungs,

Mmp9 was upregulated in IL1-KO mice by the highest dose of CNT-1 and CNT-2 and thus other mechanisms may exist to increase its expression in the lung from these mice. In addition, *Mmp13* was upregulated by CNT-1 and CNT-2 in the pleura of both WT and IL1-KO mice but only in the lung of IL1-KO mice. *Mmp13* was also increased by 162 μg MWCNT exposure in the lungs of mice after 28 days (Poulsen et al., 2015) or after oropharyngeal aspiration of 1, 2, and 4 mg/kg CNT *in vivo* (Wang et al., 2011).

Another gene greatly affected by MWCNTs and crocidolite asbestos was *Timp1*. This gene belongs to the family of tissue inhibitors of metalloproteinases (TIMPs) which are tissue-specific, endogenous inhibitors of metalloproteinases, including the MMPs. The balance between MMPs and TIMPs controls proteolysis of extracellular matrix (ECM) (Arpino, Brock, and Gill, 2015). TIMP1 has been associated with latent or pro-MMP9, but has also been found to be a strong inhibitor of many other MMPs. Expression and functional studies of TIMP1 in knockout mice showed that TIMP1 can attenuate degradation of ECM under pathological conditions and is often found in pro-fibrotic environments (Kim et al., 2005). In the present study, the *Timp1/Mmp9* ratio was highest with CNT-1 exposure. *Timp1* was increased by 162 μg of CNT in the lungs after 28 days as well (Poulsen et al., 2015). In the IL1-KO mice, *Timp1* expression was low in the mice treated with CNT-2 and asbestos. TIMP1 is found to be positively regulated by IL-1 in other studies (Wilczynska et al., 2006; Wisithphrom, Murray, and Windsor 2006; Wisithphrom and Windsor, 2006). However, a strong increase in its expression was observed in the pleura and lungs in IL1-KO mice exposed to CNT-1. As CNT-1 is the most potent inducer of changes, this may mean that *Timp1* expression is independent of IL-1 as long as the inducing factor is strong enough.

Studies on TIMP4 are limited, but there is some evidence that it acts to restrict ECM proteolysis (Arpino, Brock, & Gill, 2015). However, there is also evidence that it may do the opposite, namely decrease fibrosis (Takawale et al., 2014). In the present study, *Timp4* was downregulated by both doses of CNT-1 and the highest dose of CNT-2 and asbestos. These results may indicate that *Timp4* has an anti-fibrotic role in our model. There is still lack of evidence for the role of the balance between TIMPs and MMPs and regulation of metalloproteinase activity. Our results indicate that this balance is part of the fibrotic process induced by particle exposure *in vivo*.

Anti-apoptotic *Bcl2* was downregulated by CNT-1 in pleura and lungs from WT mice, while it was downregulated by CNT-2 and the highest dose of crocidolite asbestos as well in IL1-KO mice. *Bcl2* was not affected by the presence or absence of IL-1. Studies are inconclusive on a specific role of Bcl2 in pulmonary fibrosis as both up- and downregulation is observed, concurrently with changes in expression of the pro-apoptotic members of the Bcl2 family (Safaeian, Abed, & Vaseghi, 2014). Pro-apoptotic Fas and TNF ligand have been found on the epithelial cells on the lung epithelium and can function to cause epithelial cell death resulting in fibrosis (Todd, Luzina, & Atamas, 2012). Thus, an increase in pro-apoptotic factors may be in parallel to a decrease in Bcl2 levels to increase apoptosis in the epithelium and may add up to the excessive deposition and decreased turnover of ECM.

Serpina1a expression was also decreased after particle exposure and corresponds to a similar downregulation found in mice exposed to CNTs (Wang et al., 2011). Deficiency in *Serpina1a* is characterized by an increased risk for chronic obstructive pulmonary disease including emphysema, persistent airflow obstruction, and chronic bronchitis in adult humans (Stoller et al., 2015). Therefore, the increase in fibrosis shown in the present study may be a result of *Serpina1a* downregulation after MWCNT exposure. In summary, the changes in gene expression, in particular of those elaborated on further here, are likely to contribute to the histopathological changes after exposure of the mice.

There is growing evidence for a role of miRNAs in fibrosis of several organs. From the panel of investigated miRNAs in this study, the most significant upregulation is observed for *miR-146b*, *miR-205*, and *miR-874*, whereas *miR-1a*, *miR-133a*, *miR-200a*, and *miR-200B* are significantly downregulated. *miR-146b* expression was previously found to be upregulated in the lungs of mice with pulmonary fibrosis (Chai et al., 2016). In the present study, its' induction was the highest in pleura and lung from mice exposed to MWCNTs. The effects of functional IL-1 signaling were the most apparent for CNT-2

that led to a decrease of *miR-146b* in IL1-KO mice and crocidolite asbestos that induced an opposite regulation, namely upregulation in IL1-KO mice. IL-1β has previously been shown to have a positive effect on *miR-146b* (Perry et al., 2009) supporting this observation.

It has been shown that *miR-133a* knockout mice develops severe fibrosis and heart failure (Liu et al., 2008). Furthermore, downregulation of *miR-133a* was important for the development of myocardial fibrosis and correlated to an increase in Col1a1 (Castoldi et al., 2012). Downregulation of *miR-200a* and *miR-200B* as observed here was also shown in the lungs of mice with experimental lung fibrosis (Yang et al., 2012). Investigation of miRNA expression in lung tissue from mice exposed by pharyngeal aspiration to MWCNT (Mitsui-7) showed that *miR-147* was significantly upregulated and associated with inflammatory pathology (Dymacek et al., 2015). In our study, *miR-147* is induced by 50 μg CNT-1 in WT mice, and as vascular endothelial growth factor a (*Vegfa*) is a target of *miR-147* this corresponds to the decrease of *Vegfa* observed on the mRNA array. Furthermore, *miR-199a* was significantly upregulated after MWCNT exposure and associated with fibrosis (Dymacek et al., 2015). This miRNA was upregulated by the MWCNTs in our study in IL1-KO mice. Similarly, mothers against decapentaplegic homolog 4 (*Smad4*), which is a target of *miR-199a* (Zhang et al., 2012), was downregulated in the same mice.

The effect of the three different particle types regarding their fiber number was also considered. Our previous characterization of the CNTs showed that CNT-2 consists of 15×10^6 fibrous objects/μg material, CNT-1 of 2.8×10^6 fibrous objects/μg material and UICC Crocidolite of 2.9×10^6 fibrous objects/μg material (Arnoldussen et al., 2015). Whereas the fiber number for CNT-1 and UICC Crocidolite is pretty similar, CNT-2 contains ∼5 times more. Throughout the present study UICC Crocidolite, closely followed by CNT-2, affected histological and gene expression changes in a smaller degree than CNT-1. From this, it would be possible to conclude that fiber number may not be the most important determinant in this study, but rather a size and other physicochemical properties of the fibers.

This study has some limitations. Although the presented data show pathological effects of carbon nanotubes on pleural tissue which is the site of mesothelioma formation in humans exposed to high aspect ratio fibers (i.e. asbestos), the findings in this study cannot be directly extrapolated to humans. However, the chronic inflammatory reaction due to the presence of the fibers in the pleura may act as one of the mechanisms by which CNTs may exert their negative health effects in humans. The doses used here may not be comparable to the exposures present in the work environment. Additionally, the high doses applied directly into the pleural space may lead to a rapid buildup of fibers in the pleural space which may generate nonspecific effects and large acute inflammatory responses, as well as acute tissue injury. Since the dose of CNTs as the inducing factor used here is high, the possibility that they may generate unspecific genetic and epigenetic changes cannot be ruled out. Some of the observed gene expression changes may not reflect molecular signatures that are relevant to the pathogenesis of disease resulting from occupational exposure through inhalation in humans. We are therefore currently evaluating a long-term study using lower doses, additional CNTs, and the same mice to confirm these findings and possible induction of mesotheliomas in the pleura.

In summary, the genetic and epigenetic changes likely contribute to the histopathological changes observed in fibrosis, infiltration with mononuclear cells, and hyperplasia of mesothelial cells 28 days after injection. Although the effects of CNT-1 were the most prominent, CNT-2 induced many of the same responses indicating that despite the differences in their physicochemical properties they behave similarly in many regards. Exposed WT mice were more prone to inflammation and fibrosis than IL1-KO mice. Collectively, we suggest that IL-1 partly plays a role in the fibrotic response to MWCNTs and that the two types of MWCNT used here, in addition to crocidolite asbestos, can be ranked in the following order based on their ability to induce pathologic and genetic changes: CNT-1 > CNT-2 ≥ Crocidolite asbestos. Moreover, this study strengthens the hypothesis on similarities between MWCNTs and asbestos in the pleural space.

ORCID

Shanbeh Zienolddiny (iD) http://orcid.org/0000-0001-9747-9625

References

Arnoldussen, Y. J., A. Skogstad, V. Skaug, M. Kasem, A. Haugen, N. Benker, S. Weinbruch, R. N. Apte, and S. Zienolddiny. 2015. "Involvement of IL-1 Genes in the Cellular Responses to Carbon Nanotube Exposure." *Cytokine* 73 (1): 128–137. doi:10.1016/j.cyto.2015.01.032.

Arpino, V., M. Brock, and S. E. Gill. 2015. "The Role of TIMPs in Regulation of Extracellular Matrix Proteolysis." *Matrix Biology* 44–46: 247–254. doi:10.1016/j.matbio.2015.03.005.

Castoldi, G., C. R. Di Gioia, C. Bombardi, D. Catalucci, B. Corradi, M. G. Gualazzi, M. Leopizzi, et al. 2012. "MiR-133a Regulates Collagen 1A1: Potential Role of miR-133a in Myocardial Fibrosis in Angiotensin II-Dependent Hypertension." *Journal of Cellular Physiology* 227 (2): 850–856. doi:10.1002/jcp.22939.

Chai, J., Z. H. Li, B. Zhou, H. L. Zhu, X. Y. Xie, and X. X. Zuo. 2016. "miR-146b Expression Is Upregulated in the Lung of Pulmonary Fibrosis Mice." *International Journal of Clinical and Experimental Pathology* 9: 464–472.

Davis, J. M., J. Addison, R. E. Bolton, K. Donaldson, A. D. Jones, and T. Smith. 1986. "The Pathogenicity of Long versus Short Fibre Samples of Amosite Asbestos Administered to Rats by Inhalation and Intraperitoneal Injection." *British Journal of Experimental Pathology* 67: 415–430.

Donaldson, K., and C. A. Poland. 2009. "Nanotoxicology: New Insights into Nanotubes." *Nature Nanotechnology* 4 (11): 708–710. doi:10.1038/nnano.2009.327.

Donaldson, K., R. Aitken, L. Tran, V. Stone, R. Duffin, G. Forrest, and A. Alexander. 2006. "Carbon Nanotubes: A Review of Their Properties in Relation to Pulmonary Toxicology and Workplace Safety." *Toxicological Sciences* 92 (1): 5–22. doi:10.1093/toxsci/kfj130.

Dong, J., D. W. Porter, L. A. Batteli, M. G. Wolfarth, D. L. Richardson, and Q. Ma. 2015. "Pathologic and Molecular Profiling of Rapid-Onset Fibrosis and Inflammation Induced by Multi-Walled Carbon Nanotubes." *Archives of Toxicology* 89 (4): 621–633. doi:10.1007/s00204-014-1428-y.

Dymacek, J., B. N. Snyder-Talkington, D. W. Porter, R. R. Mercer, M. G. Wolfarth, V. Castranova, Y. Qian, and N. L. Guo. 2015. "mRNA and miRNA Regulatory Networks Reflective of Multi-Walled Carbon Nanotube-Induced Lung Inflammatory and Fibrotic Pathologies in Mice." *Toxicological Sciences* 144 (1): 51–64. doi:10.1093/toxsci/kfu262.

Erdely, A., T. Hulderman, R. Salmen, A. Liston, P. C. Zeidler-Erdely, D. Schwegler-Berry, V. Castranova, et al. 2009. "Cross-Talk between Lung and Systemic Circulation during Carbon Nanotube Respiratory Exposure Potential Biomarkers." *Nano Letters* 9 (1): 36–43. doi:10.1021/nl801828z.

Fukushima, S., T. Kasai, Y. Umeda, M. Ohnishi, T. Sasaki, and M. Matsumoto. 2018. "Carcinogenicity of Multi-Walled Carbon Nanotubes: Challenging Issue on Hazard Assessment." *Journal of Occupational Health* 60 (1): 10–30. doi:10.1539/joh.17-0102-RA.

Horai, R., M. Asano, K. Sudo, H. Kanuka, M. Suzuki, M. Nishihara, M. Takahashi, and Y. Iwakura. 1998. "Production of Mice Deficient in Genes for Interleukin (IL)-1alpha, IL-1beta, IL-1alpha/Beta, and IL-1 Receptor Antagonist Shows That IL-1beta Is Crucial in Turpentine-Induced Fever Development and Glucocorticoid Secretion." *The Journal of Experimental Medicine* 187 (9): 1463–1475. doi:10.1084/jem.187.9.1463.

Huaux, F., S. Lo Re, G. Giordano, F. Uwambayinema, R. Devosse, Y. Yakoub, N. Panin, et al. 2015. "IL-1alpha Induces CD11b(Low) Alveolar Macrophage Proliferation and Maturation during Granuloma Formation." *The Journal of Pathology* 235 (5): 698–709. doi:10.1002/path.4487.

Ishida, Y., A. Kimura, T. Kondo, T. Hayashi, M. Ueno, N. Takakura, K. Matsushima, and N. Mukaida. 2007. "Essential Roles of the CC Chemokine Ligand 3-CC Chemokine Receptor 5 Axis in Bleomycin-Induced Pulmonary Fibrosis through Regulation of Macrophage and Fibrocyte Infiltration." *American Journal of Pathology* 170 (3): 843–854. doi:10.2353/ajpath.2007.051213.

Jakubzick, C., E. S. Choi, B. H. Joshi, M. P. Keane, S. L. Kunkel, R. K. Puri, and C. M. Hogaboam. 2003. "Therapeutic Attenuation of Pulmonary Fibrosis via Targeting of IL-4- and IL-13-Responsive Cells." *Journal of Immunology* 171 (5): 2684–2693. doi:10.4049/jimmunol.171.5.2684.

Kasai, T., Y. Umeda, M. Ohnishi, H. Kondo, T. Takeuchi, S. Aiso, T. Nishizawa, M. Matsumoto, and S. Fukushima. 2015. "Thirteen-Week Study of Toxicity of Fiber-like Multi-Walled Carbon Nanotubes with Whole-Body Inhalation Exposure in Rats." *Nanotoxicology* 9 (4): 413–422. doi:10.3109/17435390.2014.933903.

Kasai, T., Y. Umeda, M. Ohnishi, T. Mine, H. Kondo, T. Takeuchi, M. Matsumoto, and S. Fukushima. 2016. "Lung Carcinogenicity of Inhaled Multi-Walled Carbon Nanotube in Rats." *Particle and Fibre Toxicology* 13 (1): 53.

Kim, K. H., K. Burkhart, P. Chen, C. W. Frevert, J. Randolph-Habecker, R. C. Hackman, P. D. Soloway, and D. K. Madtes. 2005. "Tissue Inhibitor of Metalloproteinase-1 Deficiency Amplifies Acute Lung Injury in Bleomycin-Exposed Mice." *American Journal of Respiratory Cell and Molecular Biology* 33 (3): 271–279. doi:10.1165/rcmb.2005-0111OC.

Krelin, Y., E. Voronov, S. Dotan, M. Elkabets, E. Reich, M. Fogel, M. Huszar, et al. 2007. "Interleukin-1beta-Driven Inflammation Promotes the Development and Invasiveness of Chemical Carcinogen-Induced Tumors." *Cancer Research* 67 (3): 1062–1071. doi:10.1158/0008-5472.CAN-06-2956.

Liu, N., S. Bezprozvannaya, A. H. Williams, X. Qi, J. A. Richardson, R. Bassel-Duby, and E. N. Olson. 2008. "microRNA-133a Regulates Cardiomyocyte Proliferation and Suppresses Smooth Muscle Gene Expression in the Heart." *Genes & Development* 22 (23): 3242–3254. doi:10.1101/gad.1738708.

Manicone, A. M., and J. K. Mcguire. 2008. "Matrix Metalloproteinases as Modulators of inflammation." *Seminars in Cell &Amp; Developmental Biology* 19 (1): 34–41. doi:10.1016/j.semcdb.2007.07.003.

Mercer, R. R., A. F. Hubbs, J. F. Scabilloni, L. Wang, L. A. Battelli, D. Schwegler-Berry, V. Castranova, and D. W. Porter. 2010. "Distribution and Persistence of Pleural Penetrations by Multi-Walled Carbon Nanotubes." *Particle and Fibre Toxicology* 7 (1): 28. doi:10.1186/1743-8977-7-28.

Moore, B. B., L. Murray, A. Das, C. A. Wilke, A. B. Herrygers, and G. B. Toews. 2006. "The Role of CCL12 in the Recruitment of Fibrocytes and Lung Fibrosis." *American Journal of Respiratory Cell and Molecular Biology* 35 (2): 175–181. doi:10.1165/rcmb.2005-0239OC.

Murphy, F. A., C. A. Poland, R. Duffin, K. T. Al-Jamal, H. Ali-Boucetta, A. Nunes, F. Byrne, et al. 2011. "Length-Dependent Retention of Carbon Nanotubes in the Pleural Space of Mice Initiates Sustained Inflammation and Progressive Fibrosis on the Parietal Pleura." *American Journal of Pathology* 178 (6): 2587–2600. doi:10.1016/j.ajpath.2011.02.040.

Murphy, F. A., C. A. Poland, R. Duffin, and K. Donaldson. 2013. "Length-Dependent Pleural Inflammation and Parietal Pleural Responses after Deposition of Carbon Nanotubes in the Pulmonary Airspaces of Mice." *Nanotoxicology* 7 (6): 1157–1167.

Murthy, S., A. Ryan, C. He, R. K. Mallampalli, and A. B. Carter. 2010. "Rac1-Mediated Mitochondrial H_2O_2 Generation Regulates MMP-9 Gene Expression in Macrophages via Inhibition of SP-1 and AP-1." *Journal of Biological Chemistry* 285 (32): 25062–25073. doi:10.1074/jbc.M109.099655.

Oh, H., S. Yang, M. Park, and J. S. Chun. 2008. "Matrix Metalloproteinase (MMP)-12 Regulates MMP-9 Expression in Interleukin-1beta-Treated Articular Chondrocytes."

Journal of Cellular Biochemistry 105 (6): 1443–1450. doi:10.1002/jcb.21963.

Pardo, A., S. Cabrera, M. Maldonado, and M. Selman. 2016. "Role of Matrix Metalloproteinases in the Pathogenesis of Idiopathic Pulmonary Fibrosis." *Respiratory Research* 17 (1): 23. doi:10.1186/s12931-016-0343-6.

Perry, M. M., A. E. Williams, E. Tsitsiou, H. M. Larner-Svensson, and M. A. Lindsay. 2009. "Divergent Intracellular Pathways Regulate Interleukin-1beta-Induced miR-146a and miR-146b Expression and Chemokine Release in Human Alveolar Epithelial Cells." *FEBS Letters* 583 (20): 3349–3355. doi:10.1016/j.febslet.2009.09.038.

Poland, C. A., R. Duffin, I. Kinloch, A. Maynard, W. A. Wallace, A. Seaton, V. Stone, S. Brown, W. MacNee, and K. Donaldson. 2008. "Carbon Nanotubes Introduced into the Abdominal Cavity of Mice Show Asbestos-like Pathogenicity in a Pilot Study." *Nature Nanotechnology* 3 (7): 423–428. doi:10.1038/nnano.2008.111.

Porter, D. W., A. F. Hubbs, B. T. Chen, W. Mckinney, R. R. Mercer, M. G. Wolfarth, L. Battelli, et al. 2013. "Acute Pulmonary Dose-Responses to Inhaled Multi-Walled Carbon Nanotubes." *Nanotoxicology* 7 (7): 1179–1194.

Poulsen, S., N. R. Jacobsen, S. Labib, D. Wu, M. Husain, A. Williams, J. P. Bogelund, et al. 2013. "Transcriptomic Analysis Reveals Novel Mechanistic Insight into Murine Biological Responses to Multi-Walled Carbon Nanotubes in Lungs and Cultured Lung Epithelial Cells." *PLoS One* 8 (11): e80452. doi:10.1371/journal.pone.0080452.

Poulsen, S. S., A. T. Saber, A. Williams, O. Andersen, C. Kobler, R. Atluri, M. E. Pozzebon, et al. 2015. "MWCNTs of Different Physicochemical Properties Cause Similar Inflammatory Responses, but Differences in Transcriptional and Histological Markers of Fibrosis in Mouse Lungs." *Toxicology and Applied Pharmacology* 284 (1): 16–32. doi:10.1016/j.taap.2014.12.011.

Ryman-Rasmussen, J. P., M. F. Cesta, A. R. Brody, J. K. Shipley-Phillips, J. I. Everitt, E. W. Tewksbury, O. R. Moss, et al. 2009. "Inhaled Carbon Nanotubes Reach the Subpleural Tissue in Mice." *Nature Nanotechnology* 4 (11): 747–751. doi:10.1038/nnano.2009.305.

Safaeian, L., A. Abed, and G. Vaseghi. 2014. "The Role of Bcl-2 Family Proteins in Pulmonary Fibrosis." *European Journal of Pharmacology* 741: 281–289. doi:10.1016/j.ejphar.2014.07.029.

Snyder-Talkington, B. N., J. Dymacek, D. W. Porter, M. G. Wolfarth, R. R. Mercer, M. Pacurari, J. Denvir, V. Castranova, Y. Qian, and N. L. Guo. 2013. "System-Based Identification of Toxicity Pathways Associated with Multi-Walled Carbon Nanotube-Induced Pathological Responses." *Toxicology and Applied Pharmacology* 272 (2): 476–489. doi:10.1016/j.taap.2013.06.026.

Stoller, J. K., L. S. Aboussouan, R. E. Kanner, L. A. Wilson, P. Diaz, R. Wise, and L. R. Group. 2015. "Characteristics of Alpha-1 Antitrypsin-Deficient Individuals in the Long-Term Oxygen Treatment Trial and Comparison with Other Subjects with Chronic Obstructive Pulmonary Disease."

Annals of the American Thoracic Society 12 (12): 1796–1804. doi:10.1513/AnnalsATS.201506-389OC.

Suzui, M., M. Futakuchi, K. Fukamachi, T. Numano, M. Abdelgied, S. Takahashi, M. Ohnishi, et al. 2016. "Multiwalled Carbon Nanotubes Intratracheally Instilled into the Rat Lung Induce Development of Pleural Malignant Mesothelioma and Lung Tumors." Cancer Science 107 (7): 924–935. doi:10.1111/cas.12954.

Takagi, A., A. Hirose, M. Futakuchi, H. Tsuda, and J. Kanno. 2012. "Dose-Dependent Mesothelioma Induction by Intraperitoneal Administration of Multi-Wall Carbon Nanotubes in p53 Heterozygous Mice." Cancer Science 103 (8): 1440–1444. doi:10.1111/j.1349-7006.2012.02318.x.

Takawale, A., D. Fan, R. Basu, M. Shen, N. Parajuli, W. Wang, X. Wang, G. Y. Oudit, and Z. Kassiri. 2014. "Myocardial Recovery from Ischemia-Reperfusion Is Compromised in the Absence of Tissue Inhibitor of Metalloproteinase 4." Circulation: Heart Failure 7 (4): 652–662. doi:10.1161/CIRCHEARTFAILURE.114.001113.

Timbrell, V., J. C. Gibson, and I. Webster. 1968. "UICC Standard Reference Samples of Asbestos." International Journal of Cancer 3 (3): 406–408. doi:10.1002/ijc.2910030312.

Todd, N. W., I. G. Luzina, and S. P. Atamas. 2012. "Molecular and Cellular Mechanisms of Pulmonary Fibrosis." Fibrogenesis & Tissue Repair 5 (1): 11. doi:10.1186/1755-1536-5-11.

Vaslet, C. A., N. J. Messier, and A. B. Kane. 2002. "Accelerated Progression of Asbestos-Induced Mesotheliomas in Heterozygous p53+/- Mice." Toxicological Sciences 68 (2): 331–338. doi:10.1093/toxsci/68.2.331.

Wang, X., P. Katwa, R. Podila, P. Chen, P. C. Ke, A. M. Rao, D. M. Walters, C. J. Wingard, and J. M. Brown. 2011. "Multi-Walled Carbon Nanotube Instillation Impairs Pulmonary Function in C57BL/6 Mice." Particle and Fibre Toxicology 8 (1): 24. doi:10.1186/1743-8977-8-24.

Wilczynska, K. M., S. M. Gopalan, M. Bugno, A. Kasza, B. S. Konik, L. Bryan, S. Wright, I. Griswold-Prenner, and T. Kordula. 2006. "A Novel Mechanism of Tissue Inhibitor of Metalloproteinases-1 Activation by Interleukin-1 in Primary Human Astrocytes." Journal of Biological Chemistry 281 (46): 34955–34964. doi:10.1074/jbc.M604616200.

Wisithphrom, K., P. E. Murray, and L. J. Windsor. 2006. "Interleukin-1 Alpha Alters the Expression of Matrix Metalloproteinases and Collagen Degradation by Pulp Fibroblasts." Journal of Endodontics 32 (3): 186–192. doi:10.1016/j.joen.2005.10.055.

Wisithphrom, K., and L. J. Windsor. 2006. "The Effects of Tumor Necrosis Factor-Alpha, Interleukin-1beta, Interleukin-6, and Transforming Growth Factor-beta1 on Pulp Fibroblast Mediated Collagen Degradation." Journal of Endodontics 32 (9): 853–861. doi:10.1016/j.joen.2006.03.017.

Xu, J., M. Futakuchi, H. Shimizu, D. B. Alexander, K. Yanagihara, K. Fukamachi, M. Suzui, et al. 2012. "Multi-Walled Carbon Nanotubes Translocate into the Pleural Cavity and Induce Visceral Mesothelial Proliferation in Rats." Cancer Science 103 (12): 2045–2050., doi:10.1111/cas.12005.

Yang, S., S. Banerjee, A. De Freitas, Y. Y. Sanders, Q. Ding, S. Matalon, V. J. Thannickal, E. Abraham, and G. Liu. 2012. "Participation of miR-200 in Pulmonary Fibrosis." The American Journal of Pathology 180 (2): 484–493. doi:10.1016/j.ajpath.2011.10.005.

Zhang, Y., K. J. Fan, Q. Sun, A. Z. Chen, W. L. Shen, Z. H. Zhao, X. F. Zheng, and X. Yang. 2012. "Functional Screening for miRNAs Targeting Smad4 Identified miR-199a as a Negative Regulator of TGF-Beta Signalling Pathway." Nucleic Acids Research 40 (18): 9286–9297. doi:10.1093/nar/gks667.